Available online at www.sciencedirect.com

SCIENCE DIRECT®

Journal of Geochemical Exploration 84 (2004) 105–125

JOURNAL OF GEOCHEMICAL EXPLORATION

www.elsevier.com/locate/jgeoexp

Geology and geochemistry of the Shangmanggang red clay-type gold deposit in West Yunnan

Rao Wenbo[a,*], Gao Zhenmin[a], Yang Zhusen[a,b], Luo Taiyi[a]

[a] *Institute of Geochemistry, Chinese Academy of Sciences, 73 Guanshui road, Guiyang 550002, China*
[b] *Institute of Mineral Resources, Chinese Academy of Geological Sciences, Beijing 100052, China*

Received 4 July 2003; accepted 29 April 2004
Available online 4 July 2004

Abstract

The Shangmanggang red clay-type gold deposit was discovered in West Yunnan in the early 1990s, which is strictly controlled by the Shangmanggang fault, belonging to a new type of gold deposits. Its red clay profile, about 20 m thick, is divided into six zones: topsoil zone, slope-wash zone, travertine zone, eluvium zone, saprolite zone, and unweathered bedrocks. The degree of laterization is relatively high in the eluvium zone where gold is very rich. Ore minerals mainly consist of quartz, goethite, and clay minerals. Sand and silt fractions are mainly composed of quartz and goethite with minor feldspar; clay fractions comprise illite, kaolinite, quartz, a small quantity of goethite, feldspar, and hydrargillite. The variation of gold content in the red clays is similar to that of sand fractions. Gold is probably closely associated with iron nodules developed in the red clays. At the same time, gold is well correlated with clay minerals and Fe, Mn oxides. Gold exists mostly in the form of dissociated gold and microfine gold, which is adsorbed on the surface or in the cracks of quartz, clay minerals, and goethite. Geochemistry characteristics of the major elements, trace elements, and REEs in the red clays of the Shangmanggang red clay-type gold deposit in West Yunnan were studied in detail. The results show that Al_2O_3, Fe_2O_3, and K_2O were migrated and precipitated together in the red clay profile, but the case is not true for SiO_2. As a whole, SiO_2 is high in content, desilication is incomplete, and the degree of laterization is low in the red clays, except for a high degree of laterization in the eluvium zone. In contrast with the sedimentary rocks and altered rocks, the red clays come from the Mengga Formation mudstone with laterization. Au, Hg, As, Sb, Cu, Pb, Zn, and Mo are coextensive trace elements in the red clay profile and are significantly enriched in the eluvium zone where laterization is relatively complete. The crust-normalized large-ion-lithophile element patterns in the red clays are similar to those of both altered rocks and the Mengga Formation. The chondrite-normalized REEs patterns in the red clays are also similar to those of both altered rocks and the Mengga Formation. The LREEs are enriched, and gold is concentrated in the location where REE fractionation is strong. Our work reveals that gold comes mainly from the altered rocks, and the red clays are mainly derived from the Mengga Formation and altered rocks.

Keywords: Red clay-type gold deposit; Red clay weathering profile; Gold; Major element; Trace element; REE; Source of ore-forming materials; Shangmanggang (SMG); Yunnan

1. Introduction

In the early 1980s, a new type of gold deposit was discovered in Boddington, Western Australia (Davy

* Corresponding author.
E-mail address: raowenbo@163.com (R. Wenbo).

0375-6742/$ - see front matter © 2004 Elsevier B.V. All rights reserved.
doi:10.1016/j.gexplo.2004.04.001

and El-ansary, 1986), and Igarape Bahia, Brazil (Zang and Fyfe, 1993), which was called lateritic gold deposit due to the ore existing in the lateritic profile. This type of gold deposit is characterized by low grade, large scale, easy exploitation, and dressing. Subsequently, many lateritic gold deposits were discovered in many parts of the world, such as Fijian (Webster and Mann, 1984), USA (Heylmun, 1986), Guyana (Taylor et al., 1989), Sierra leone (Davies et al., 1989), Niger (Gleeson and Poulin, 1989), Mali (Freyssinet et al., 1989a), Cameroon (Freyssinet et al., 1989b), Gabon (Lecomte and Colin, 1989; Colin and Vieillard, 1991), Vietnam (Shcherbakov et al., 1992), India (Santosh and Omana, 1991; Narayanaswamy and Krishnakumar, 1996), and other areas of Australia and Brazil (Glasson et al., 1988; Freyssinet et al., 1990; Porto and Hale, 1995, 1996) because of their high benefits.

Like lateritic gold deposits, many hypergenic gold deposits that exist in the red regolith have been found extensively in many provinces of South China since the late 1980s, such as Hubei Province (Li, 1993), Hunan Province (Jiang, 1999; Hong et al., 1996), Yunnan Province (Zhang, 1998; Lu, 1994), Guangxi Province (Wang, 1999), Guizhou Province (Liu, 1999), Jiangxi (He, 1998), and Jiangsu Province (Qiu and Chen, 1998). These gold deposits are similar to lateritic gold deposits in mineralization background as follows: (1) relatively stable tectonic condition with immobile groundwater table and stable supply system of surface water and groundwater; (2) source of ore-forming materials such as primary gold ore and altered rocks containing high gold content; (3) humid and hot climatic conditions with sufficient rainfall; (4) geomorphology of peneplain, low hill, knap, and karst; (5) Tertiary and Quaternary mineralization epoch.

Although the mineralization background is similar, many characteristics of the hypergenic gold deposits in China are obviously different from those of the lateritic gold deposits as described below. Therefore, these gold deposits in China are named as the red clay-type gold deposits. The differences between the red clay-type gold deposit and lateritic gold deposit are as follows:

(1) In these gold deposits in China (No.4 Geological Party of HBGMR, 1994; Chen, 1999), SiO_2 is more than 55% in content, and the Fe_2O_3 content is below 20%. In lateritic gold deposits (Zang and Fyfe, 1993; Davy and El-ansary, 1986; Carvalho et al., 1991; Costa and Araújo, 1996; Davies et al., 1989), the SiO_2 content is below 45%, the Fe_2O_3 content is above 20%, and the Al_2O_3 content is below 35%. Compared with lateritic gold deposits, the red clay-type gold deposits in China show incomplete hypergenic weathering and silicification.

(2) Profiles of the majority of the red clay-type gold deposits in China are poorly developed and usually thin. Soil delamination is unconspicuous, ore layer containing gold is loose in texture, and gold mainly comes from gold-containing parent rocks in these red clay profiles. However, the profiles of lateritic gold deposits abroad are much thicker and developed completely (Davy and El-ansary, 1986; Costa, 1993). The lateritic profile is typically divided into six zones from the top to the bottom: topsoil zone, ferruginous zone, mottled zone, mottled clay zone, saprolite, and bedrock.

(3) Southern China (especially southwestern China) belongs to the subtropical zone where climatic conditions are favorable to the occurrence of laterization. Cenozoic tectonic activities are violent and frequent in southern China where such geomorphologic features as mountains and hills are widely developed, topography is intensely incised, peneplainization is incomplete, and groundwater tables fluctuate strongly. Because of these factors mentioned above, many gold deposits of this type are of incomplete oxidation, weathering, and leaching. Lateritic gold deposits abroad usually occur in tropic, subtropic zones undergoing violent laterization and oxidation with strong desilication under the condition of peneplain and steady groundwater table.

(4) Ores of the red clay-type gold deposits in China still contain many clay minerals in which there are a small number of Fe (Al) oxides and minor gibbsite, and generally, kaolinite coexists with illite (Hong et al., 1996; Liu, 1996). Minerals in lateritic gold deposits are dominated by Fe (Al) oxides or (and) hydroxides. Clay minerals occur under lateritic layers, dominated by kaolinite, with gibbsite commonly seen.

(5) Ore-hosted layers in the lateritic gold deposit mainly exist in the ferruginous zone and the upper part of the clay zone. Ore-hosted layers exist exclusively in the red clay zone, and the bonanza is seriously affected by topography in the red clay-type gold deposits in China.

(6) Gold in the red clay-type gold deposits is mostly natural gold and electrum, microfine or submicro-fine, which is adsorbed and enclosed by goethite and clay minerals. On account of the adsorption and enclosure of microfine gold by clay minerals, the lixiviation ratio of gold is low in some mines (Jin et al., 1995). Gold is correlated with Fe (Al) oxides and hydroxides, and its lixitation ratio is high in lateritic gold deposits. Natural gold or doggie gold usually occurs in the lateritic profile and the purity and fineness of gold change from one profile to another (Mann, 1984; Freyssinet et al., 1989a). Erosion signals are often observed on the surface of gold in lateritic gold deposits, indicating that gold was transported and reprecipitated, whereas argent was leached to result in increasing purity of gold.

(7) Source materials of the red clay-type gold deposit in China are mainly sedimentary rocks and primary gold deposits. Bedrocks of the lateritic gold deposits may be magmatic rocks, metasedimentary rocks, or metamorphic rocks showing great variations in lithology.

(8) The red clay-type gold deposits in China are mostly small or medium in scale with a high grade of gold, especially in these gold deposits occurring in karst terrains. Lateritic gold deposits are mainly large or super large in scale with a low grade of gold.

(9) The Shangmanggang (SMG) gold deposit was discovered by the Geological Surveying Team of Yunnan, Nuclear Industry Department in Luxi district, Southwest Yunnan Province in the early 1990s. This gold deposit belongs to the red clay-type gold deposit, one of the newly industrial types in Southwest China since 1990. It is characterized by a high grade, shallow depth of burial, medium scale, and great benefits from exploitation. In this paper, the geological characteristics of the SMG gold deposits are introduced, and material compositions and element geochemistry are presented in detail.

2. Geology

Located 37 km south of Luxi City, Southwest Yunnan, the SMG red clay-type gold deposit is situated in the contact zone of the Luxi fold bundle and Hushui-Longchuan fold bundle, which belong to the Fugong-Zhenkang fold zone, the second-order structure unit of the Gangdise-Nianqingtanggula Mountains fold series. These two fold bundles are separated by the Longling-Ruili Fault spreading northeastwards. On the northwestern flank of the Longling-Ruili Fault, the Hushui-Longchuan fold bundle is composed of green schist to amphibolitic metamorphic rocks of Proterozoic Gaoligong Group and Mesozoic granodiorite. On the southeastern flank, the Luxi fold bundle consists of low-grade metamorphic clastic rocks of Sinian-Cambrian Gongyanghe Group, Permian dolomite, and Jurassic red mudstone and siltstone. Five second-order faults parallel to Longling-Ruili Fault are developed northeastwards on the southeastern flank, i.e., the Zhichang fault, the Xiamanggang fault, the Shangmanggang fault, the Hule fault, and the Yingpanshan fault (Fig. 1). The SMG gold deposit is at the northeastern end of the 20-km-long Shangmanggang fault, which trends to NW. Compressive shearing at the early stage and tensile faulting at the late stage resulted in the formation of a fractured zone, measured at 100–300 m in width, which consists of cataclastic rocks, granulitic rocks, and fault gouge, as well as tectonic breccia. Hydrothermal alterations along the SMG fault were well developed with jasperoid, dickite–kaolinite, hydromica, carbonate, barite, pyrite, stibnite, hematite, cinnabar, and sphalerite. Altered rocks usually contain gold, providing the basis for the formation of primary Carlin-type gold ore bodies locally, which are the main material source of the SMG red clay-type gold deposit. The northwestern part of the SMG fault is composed of mudstones, sandstones, and calcic siltstones interbedded with limestones of the Middle Jurassic Mengga Formation, while the southeastern part is composed of dolomite and dolomic limestone intercalated with limestone of the Low Permian Shazipo Formation. The SMG red clay-type gold deposit is strictly controlled by the SMG fault, which extends northeastwards. The mineralized zone is about 7-km length in total and is divided into four sections: Guoyuan section, Maiwoba section, Guanglingpo section, and the Yangshishan section. Ore bodies in the SMG red clay-type gold deposit are platy and lenticular in shape (Fig. 2), and are hosted in the red

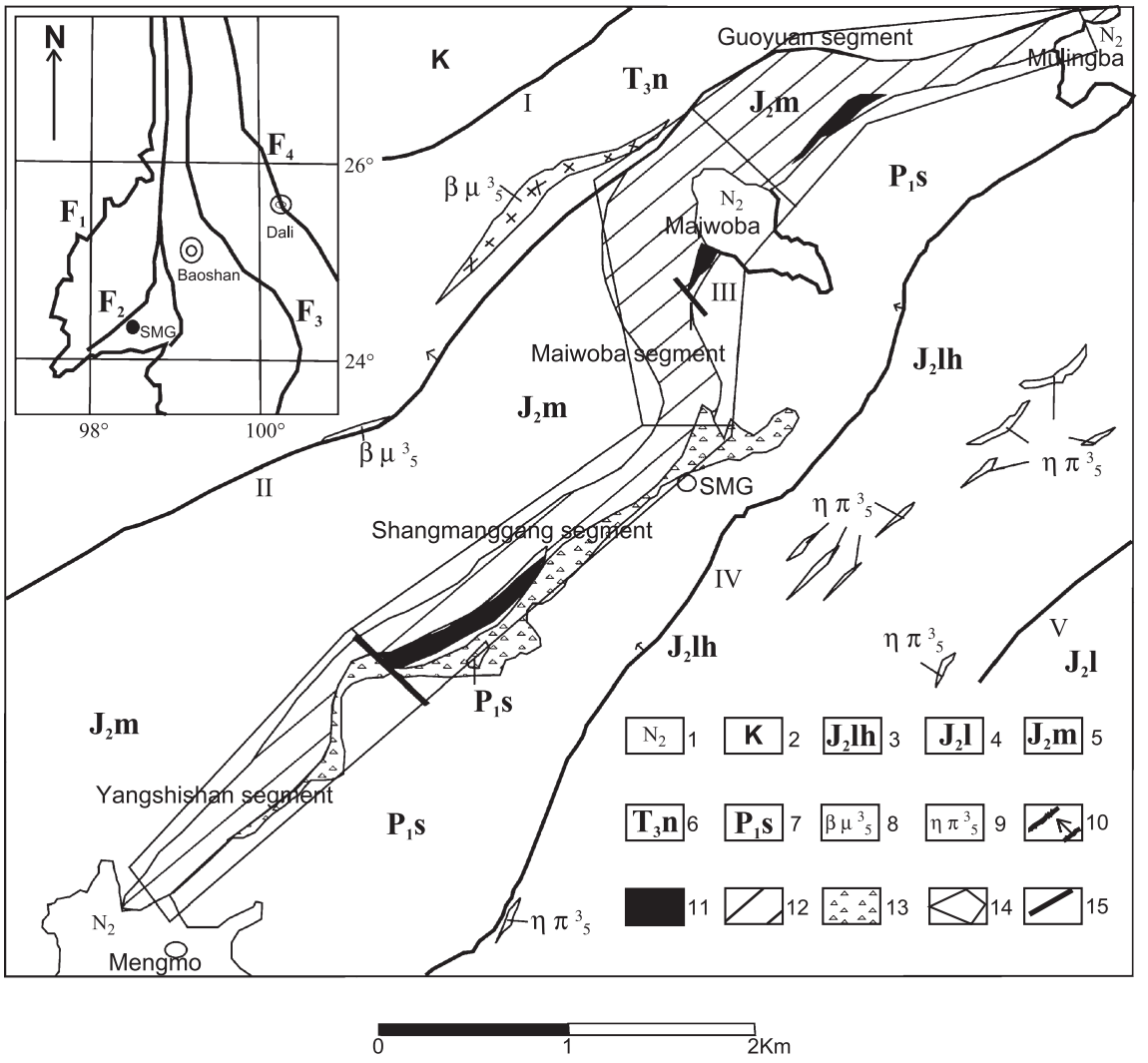

Fig. 1. Geological sketch map of the Shangmanggang gold ore district. 1—Pliocene; 2—Cretaceous; 3—Mid-Jurassic Longhai Formation; 4—Mid-Jurassic Liuwai Formation; 5—Mid-Jurassic Mengga Formation; 6—Early Triassic Nanshuba Formation; 7—Low-Permian Shazipo Formation; 8—diabase; 9—monzonite porphyry; 10—Fault and direction; 11—Silicification zone; 12—Clayization zone; 13—Karst collapse breccia; 14—Range of ore district; 15—Small faultage; I—Zhichan fault; II—Xiamanggang fault; III—Shangmanggang fault; IV—Hule fault; V—Yingpanshan fault; F_1—Nu River Fault; F_2—Longling-Ruili Fault; F_3—Lancang River Fault; F_4—Jingsha River-Hong River Fault.

clays accumulated on the karst-eroded surface of the Shazipo Formation near the SMG fault. Mineralization is homogeneous, and reserves are moderate in scale. In addition, monzonite–porphyry, diabase, and lamprophyre dykes were intruded along the SMG fault during the Late Yanshan period; of these, only a few veins of lamprophyre dykes are exposed in the Yangshishan segment of the mining district.

3. Samples and methods

3.1. Sampling

Various types of rocks of the SMG red clay-type gold deposit were sampled in the mining district. Samples of the red clays were collected from the Guanglingpo ore run. Three lateral lines in the red

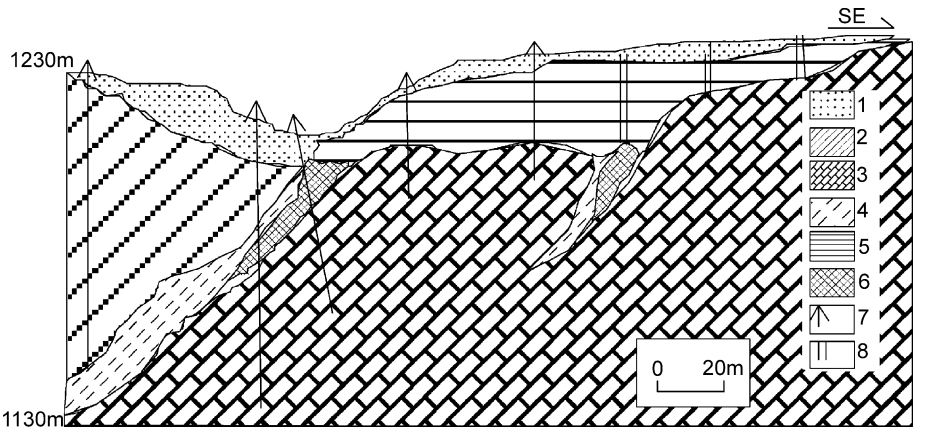

Fig. 2. Geological section of the Shangmanggang gold deposit. 1—Quaternary; 2—Mid Jurassic Mengga Formation mudstone; 3—Low Permian Shazipo Formation dolomite; 4—compresso-fractured zone of Shangmanggang Fault; 5—Red clay-type gold deposit; 6—Carlin-type gold deposit; 7—Drilling core; 8—shallow well.

clay profile were selected at intervals of 5 m. Samples were collected from the top to the bottom by chiseling flute. Then, samples from the same zones of the three lines in the red clay profile were mixed, and each sample was reduced in mass to about 1 kg by quartering. In addition, seven samples of altered rocks were collected in the Guanglingpo and Maiwoba ore runs. Nineteen sedimentary rock samples were collected in the SMG ore district; three samples of magmatic rocks were collected in Xishan and Feihong near the SMG ore district and in the Yangshishan ore run. After air drying at room temperature, red clay samples were ground in an agate mortar to a size fraction as fine as 0.149 mm and preserved.

3.2. Analytical methods

3.2.1. Grain size fraction of the red clays

Samples of the red clays (S111, S112, S113, S114, S115, and S116) were taken (150 g each) and divided into five fractions by wet sieving and sedimentation-siphonating methods (Zhao and Zhang, 1990): >900 μm, 900–150 μm, 150–76 μm, 76–2 μm, and <2 μm. The <2 μm fractions were separated from samples S119, S118, and S117 by the sedimentation-siphonating method.

3.2.2. Chemical analysis

Rocks and different fractions of the red clays were analyzed for gold by atomic absorption spectrophotometry (AAS), and the major elements were analyzed after routine wet chemistry in the Institute of Geochemistry, Chinese Academy Sciences. Analytical uncertainties are ± 2% for all major elements, less than ± 5% for gold.

3.2.3. Lixiviation of gold

About 50 g of each red clay sample was weighed (S111–S116) and put into a 500-ml tapered bottle. An admixture of NaCN and NaOH was added (about 250 ml) into each tapered bottle to get a ratio of solid to liquid (1:5). The solutions were put aside for about 12 h, then shaken for 8 h. Oxygen was put into each bottle once every 4 h. The solutions were separated centrifugally to get clean liquid and residues, the clear liquid and residues were measured for gold by AAS after input of 5ml NaClO and some quantities of nitrohydrochloric acid.

3.2.4. X-ray diffraction

The <2 μm and 76–2 μm fractions were analyzed for mineral compositions by using Fully automatical X-ray diffraction apparatus (D/Max-2200) in the Institute of Geochemistry, Chinese Academy Sciences. The following instrument conditions were observed: ① accuracy of the angle tester was better than 0.02°; resolution of the apparatus was better than 60%; the total stability was better than ± 1%; ② Cu–Kα radiation; ③ scattering slit and emission slit was 1°, and acceptor slit was 0.15 mm; ④ scanning speed:

6°–8°/min; ⑤ sampling width: 0.02° or 0.04° (2θ); ⑥ working voltage: 40 kV; ⑦ working electrical current: 20 mA; and ⑧ scan range: 2°–70° (2θ).

3.2.5. ICP-MS

About 50 mg of each sample was weighed and put into a Teflon airproof decomposer made in the ore geochemistry laboratory. HF (1 ml) and 1 ml HNO_3 were added to the Teflon container which was heated in an oven at about 190 °C for about 12 h. After removal, the liquid was evaporated to dryness on a platen heater at low temperature. The above procedure was repeated twice. Finally, the residues were placed into 50-ml plastic bottles with 2 ml HNO_3 and 5 ml H_2O. Rh was used as the internal standard. Trace elements and rare earth elements were measured by ICP-MS in the Institute of Geochemistry, Chinese Academy Sciences. Standard Reference Materials are NBS-1633 and SY-4. Analytical uncertainties are below ±10% for REEs and less than ±5% for other trace elements.

4. Description of the red clay profile

The red clays of the SMG red clay-type gold deposit resulted from incomplete weathering of parent rocks are about 20 m in thickness. This red clay profile is divided into six zones from the top to the bottom (Fig. 3):

(1) Topsoil zone: The topsoil zone is about 0–1 m thick and is composed of greyish to brown kaolin clay and humus.
(2) Slope-wash zone: the slope-wash zone is 4–8 m thick and shows development of yellow-brown clays and some pale white pipelike kaolin clays. Mengga Formation mudstone and siltstone are around 10% of the whole rocks, and sand composed of quartz, plagioclase, dickite vein and hydrothermally altered siliceous rocks is about 40%.
(3) Travertine zone: travertine zone, 0–4 m thick, comprises grey clays and lenticular travertine with minor quartz and plagioclase. Black carbonaceous clay and sand composed of 20% quartz, 5% mudstone, silicalites, and dickite veins occur in the red clays of the Guanglingpo ore run. There are large amounts of plant fragments, minor amounts of fragments of diatom, and rodentia skeleton in the red clays.
(4) Eluvium zone: the eluvium zone is up to 8 m thick in karst funnels and characterized by fuchsia sand clays mainly composed of Quartz, illite, and kaolinite. Hematite and goethite account for 20–30%, and quartz sand is around 10% in the upper part. Hematite gradually disappears and goethite decreases toward the bottom where quartz sand arrives at about 30% with 10–20% rhomboidal silt consisting of quartz sandstone, mudstone, silicified and argillized sandstone, and dickite veins.
(5) Saprolite zone: the saprolite zone is up to 8 m thick in the karst funnels, which were mainly filled by weathered karstic collapse breccias of altered rocks and Jurassic sedimentary rocks. The mineral assemblages mainly consist of illite, kaolinite, and goethite with large amounts of relicts of primary quartz and plagioclase. However, the zone is less than 1 m thick without weathered breccias, composed of loose sand clays resulted from weathering of Permain dolomite in the southeastern flank of the SMG fault.
(6) Unweathered bedrocks: unweathered bedrocks are the Permian dolomite and Jurassic mudstone and siltstone near the SMG fault; along which, alteration and mineralization occur. The altered rocks consist of quartz, carbonate, kaolin clays, barite, and minor amounts of sulfides (pyrite, stibnite, sphalerite, and cinnabar). Gold content is very low in sedimentary rocks, 0.39 to 9.35 ppm in silicified and argillized rocks, and about 9.8 ppm in silicalites, whereas up to 32.47 ppm in the location pyrite is enriched.

From the viewpoint of mineralization, the eluvium and saprolite zones were formed at the early stage of mineralization, containing main parts of the ore body. The travertine, slope-wash, and topsoil zones are of accumulation origin, because the travertine and slope-wash materials accumulated at the late stage of mineralization with comparatively weak laterization after the weathering crust were partly denuded at the early stage. Goethite, clay minerals (illite and kaolinite), and quartz are major minerals containing gold, and anatase, epidote, carbonate, and pyrite are minor minerals containing gold in the red

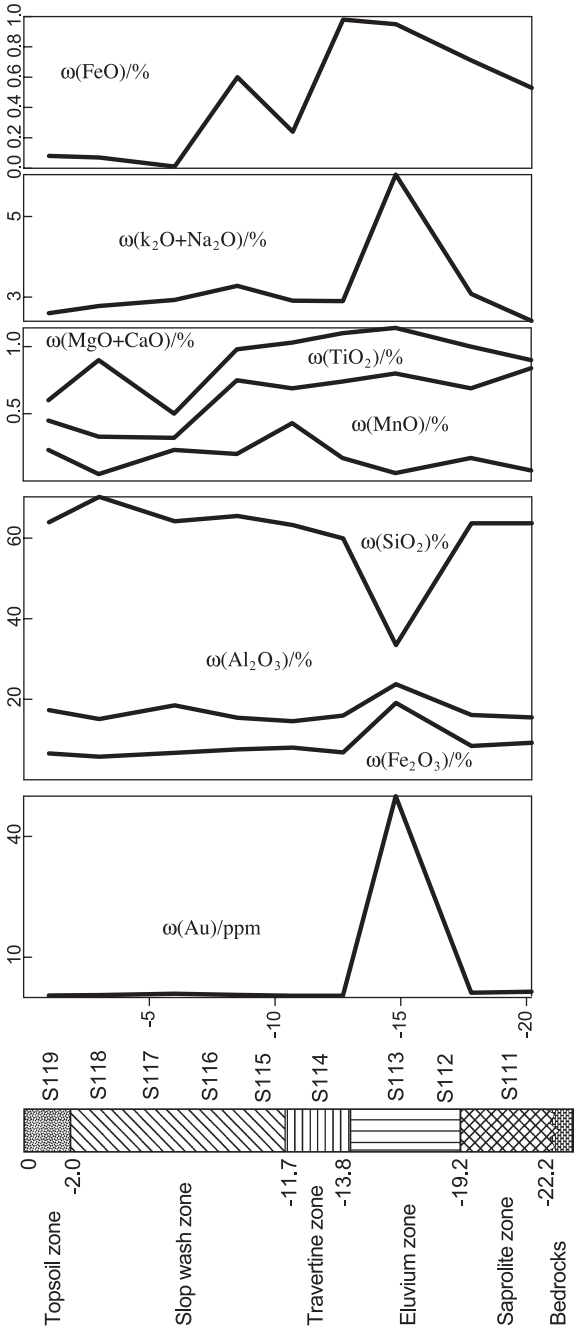

Fig. 3. Variations in contents of major elements (%) and gold (ppm) with depth (m) in the red clay profile.

Table 1
Proportions of different grain size fractions of the red clays (%) in the Guanglingpo section, Shangmanggang gold deposit

Sample no.	>900 μm	900–150 μm	150–76 μm	76–2 μm	<2 μm	Loss
S116	13.667	13.533	8.4	47.467	15.667	1.266
S115	14.1	19.127	9.8	39.133	17.84	0
S114	14.967	16.667	8.553	32.053	26.507	1.25
S113	61.367	8.133	5.647	17.047	7.093	0.713
S112	18.067	12.987	6.873	40.487	21.04	0.546
S111	15.933	13.1	6.073	43.94	20.213	0.741

clays. These minerals containing gold mainly exist in the eluvium zone.

5. Grain size fractions and mineral compositions of the red clays

5.1. Grain size fractions

Grain size fractions of the red clays were shown in Table 1. The >900 μm fraction is greatly enriched in the middle part of this profile, whereas obviously decreases toward the upper part and bottom of the profile. The 150–76 μm fraction fluctuates slightly low in the eluvium zone, but gradually increases toward the top and bottom of the profile. The 900–150 μm, 76–2 μm, and <2 μm fractions change in the same manner as the 150–76 μm fraction, although more obviously. The <2 μm fraction changes most sensitively. Its content is very low in the eluvium zone (S113), high in the travertin zone and saprolite zone, and low in both the slope-wash zone and the unweathered bedrock zone.

5.2. Mineral compositions

Observed under microscope, X-ray diffraction and transmission electrical microscope, ore minerals from the SMG red clay-type gold deposit mainly consist of goethite, clay minerals, and quartz. X-ray diffraction analysis was made on the 76–2 μm and <2 μm fractions (Table 2 and Fig. 4). Clay minerals are dominated by illite and kaolinite, with minor plagioclase, geothite, and quartz. Plagioclase is the probable weathering residue. Goethite and quartz are mostly adsorbed on clay minerals. The main mineral of the 76–2 μm fraction is quartz with a few clay minerals (Table 2) owing to coarse grains and limited decentralization of clay minerals, and this phenomenon is especially obvious in the eluvium zone, namely, quartz content is low and clay mineral is relatively high in content.

6. Distribution and lixiviation experiment of gold

6.1. Gold content in the red clays and different type of rocks

Gold content in the red clay profile changes from low to high then to low with increasing depth (Table

Table 2
Mineral contents (%) in clay and silt fractions of the red clays in the Guanglingpo section, Shangmanggang gold deposit

Grain size fractions	Sample no.	I	K	Q	B	M	Ab	Go	Or	Hy	Ch	An
<2 μm fraction	S119	28.84	23.47	1.55		7.96		11.53	9		1.73	4.73
	S118	34.38	16.96	18.73				13.09	10.22		1.44	5.18
	S117	35.35	18.58	7.72		3.78		11.80	17.12			5.66
	S116	42.8	20.17	6.94			13.32	6.95		2.69	2.93	4.20
	S115	36.78	22.52	11.06			13.09	8.13			4.23	4.19
	S114	36.79	25.31	12.24			11.97	5.46			3.51	4.67
	S113	63.03	16.99		3.32		9.04	7.61				
	S112	37.95	33.90	17.22			7.75	4.02			2.17	3.98
	S111	31.25	35.33	7.49	4.75	4.79	10.15	6.21				
76–2 μm fraction	S116	11.10	16.62	70.03								2.25
	S115	13.48	23.18	62.67								1.26
	S114	8.29	13.64	76.69								1.39
	S113	50.32	16.67	6.65			12.19		15.97			4.85
	S112	11.61	22.74	65.65								
	S111	7.25	21.13	70.56								1.06

I (illite), K (kaolinite), Q (quartz), B (brookite), M (smectite), Ab (plagioclase), Go (goethite), Or (orthoclase), Hy (gibbsite), Ch (chlorite), An (anatase); X-ray diffraction Lab of Institute of Geochemistry, Chinese Academy of Sciences.

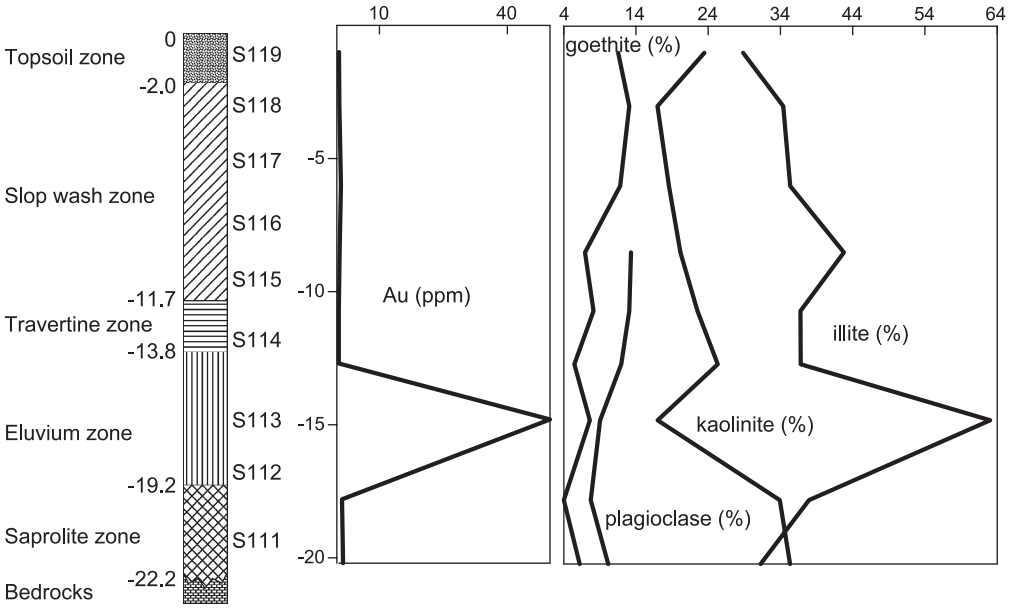

Fig. 4. Variations in contents of gold (ppm) and ore minerals (%) from the <2 μm fraction in the red clay profile.

3; Fig. 3). Gold content is below 1 ppm in the upper part (topsoil zone, slope-wash zone, and travertine zone), but above 1 ppm in the lower part of the profile (eluvium zone, saprolite zone, and bedrock zone). The highest gold content is produced in the eluvium zone. Gold content is 0.1 ppm in kaolinitization–pyritization-altered rocks, but is above 2 ppm in other altered rocks and primary ores. The highest

Table 3
Gold contents (ppm) in the red clays, altered rocks, sedimentary, rocks and magmatic rocks in the Shangmanggang gold deposit

Red clays				Altered rocks or primary ores		Sedimentary rocks		Magmatic rocks	
Depth (m)	Zones	Sample no.	Au	Rocks or ores	Au	Rocks or ores	Au	Rocks or ores	Au
1–2	Topsoil zone	S119	0.50	Carlin-type gold ore	9.80	Mudstone of Jurassic	0.13	Peridotite	0.0367
2–11.7	Slope-wash zone	S118	0.56	Silicification–pyritization mudstone	2.34	Dolomite of Permian	0.05	Basic rock vein	0.0347
		S117	0.93	Silicification-altered rock	2.12	Brecciated dolomite	0.04	Lamprophyre	0.0336
		S116	0.65	Kaolinitization–pyritization-altered rock	0.10	Grey dolomite	0.06		
		S115	0.45			Muddy dolomite	0.10		
11.7–13.8	Travertine zone	S114	0.45			Coarse-crystal dolomite	0.01		
13.8–19.2	Eluvium zone	S113	50.00						
		S112	1.17						
19.2–22.2	Saprolite zone	S111	1.43						

Table 4
Gold content (ppm) and proportion (%) in different grain size fractions of the red clays in the Guanglingpo section, Shangmanggang gold deposit

Grain size fraction (μm)	Slop-wash zone				Travertine zone		Eluvium zone				Saprolite zone	
	S116		S115		S114		S113		S112		S111	
	Au content	Au proportion	Au content	Au proportion	Au content	Au proportion	Au content	Au proportion	Au content	Au proportion	Au content	Au proportion
>900	1.88	25.50	1.46	19.25	1.46	21.02	51.9	83.59	3.38	40.06	2.55	22.92
150–900	1.18	15.81	1.20	21.60	1.18	19.86	35.1	7.49	1.34	11.42	2.17	16.25
150–76	1.48	9.08	1.02	9.62	1.19	8.33	16.1	2.07	0.85	0.58	1.30	5.12
76–2	0.83	14.00	0.83	18.11	0.70	28.04	8.88	2.21	0.86	25.36	1.14	27.04
<2	1.24	35.61	1.15	31.42	1.08	22.75	14.8	4.64	1.94	22.58	2.53	28.67

Analysis-testing Center of Institute of Geochemistry, Chinese Academy of Sciences.

gold content of sedimentary rocks is 0.13 ppm, lower than that of altered rocks and primary ores. Compared with the three types of rocks mentioned above, gold content of magmatic rocks is the lowest (Table 3).

6.2. Gold proportions in different fractions

Variation of the >900 μm fraction is very similar to that of gold in the red clay weathering profile (Tables 1 and 3). Therefore, gold content increases with increase of the >900 μm fraction, because many iron nodules are probably developed in the red clays containing gold (Li, 1998), and gold is adsorbed on iron nodules of coarse granules.

Gold proportions of different grain size fractions in the Guanglingpo ore run, Shangmanggang district were showed in Table 4. Gold proportion is the highest in the >900 μm fraction and secondly in the clay and silt fractions on the whole. The >900 μm fraction mainly consists of quartz and goethite nodules. The surface of quartz is also covered by pellicles of Fe, Mn oxides. Gold in the >900 μm fraction is probably adsorbed by Fe, Mn oxides. But, gold in the <2 and 76–2 μm fractions is mainly adsorbed by clay minerals and a few Fe, Mn oxides. Synchronous change of gold and illite in content in the red clay weathering profile also demonstrates the above result (Fig. 4). Therefore, gold has close relations with quartz, goethite, and clay minerals in the red clays.

Table 5
Gold content and proportion in different phases of the primary ores in the Shangmanggang gold deposit

Gold in different minerals	Content (ppm)	Percentage (%)
Monocase-gold grain	0.50	14.04
Linked gold grain	2.25	63.20
Gold in carbonatite	0.10	2.81
Gold in Mn minerals	0.05	1.40
Gold in pyrite	0.28	7.87
Gold in arsenopyrite	0.18	5.06
Gold in hematite and limonite	0.075	2.11
Gold in silicate	0.075	2.11
Gold inclusion in quartz	0.05	1.40
Total	3.56	100

6.3. Phase analysis of ore minerals

Phase analysis of ore minerals in the SMG red clay-type gold deposit conducted by the Geology Surveying Team of Yunnan, Nuclear Industry Department (Table 5)[1] shows natural gold is about 77.24%, mainly presented as monocase gold and linked gold, whereas there is very low percentage of gold in other minerals such as pyrite, quartz, and carbonate minerals. Phase analysis of ore minerals in the Shewushan red clay-type gold deposit shows that naked gold at a submicro fine scale is around 89.44%, but gold included in sulfides and silicates is 3.42% and 7.14%, respectively (Liu, 1996). These results indicate that gold in the red clay-type gold deposit is mostly natural, occurring on the surface or within the fissures of minerals (goethite, clay minerals, and quartz) at a submicro fine scale, and only a

[1] Geological Surveying Team of Yunnan, Nuclear Industry Department.Exploration report of the Guanglingpo ore run in the Shangmanggang gold deposit, West Yunnan 1991–1993.

Table 6
Au lixiviation of the red clays in the Shangmanggang gold deposit (%)

Sample no.	Gold in clear liquid	Gold in residues
S111	97.94	2.06
S112	98.142	1.858
S113	95.366	4.634
S114	94.349	5.651
S115	96.29	3.71
S116	94.264	5.736

minor amount of gold occurs in the interlayers of sulfides or silicates as gold inclusions or as complex compounds.

6.4. Gold lixiviation experiment

The lixiviation ratio of gold in the SMG red clay-type gold deposit is over 94% (Table 6). The lixiviation ratio of gold in the Shewushan red clay-type gold deposit in Hubei province reaches 97.21% after ore minerals was eluviated by compound solution of NaOH and NaCN for four days (No.4 Geological Party of HBGMR, 1994). Lixiviation ratio of gold in the Laowanchang red clay-type gold deposit in Guizhou province was about 98% (Chen and Yang, 1998). Therefore, the lixiviation ratio and rate of gold in the SMG gold deposit are as high as those of the Shewushan and Laowanchang gold deposits, implying most gold in the red clays is naked and natural at submicro fine scale.

7. Element geochemistry

7.1. Major element geochemistry

7.1.1. Vertical distribution of major elements in the red clay profile

Different major elements vary differently from one another in the SMG red clay-type gold deposit (Table 7; Fig. 3). Main major elements vary obviously in the upper eluvium zone as compared with in other zones; SiO_2 decreases obviously and Fe_2O_3 and Al_2O_3 increase in content. However, SiO_2 and Al_2O_3 do not change basically with slight increase of Fe_2O_3 in the other parts of the red clay profile. These above characteristics indicate that twice accumulation–laterization processes happened in the whole red clay profile. The eluvium zone was formed during the first accumulation–laterization process, during which, the upper eluvium zone was altered violently. The travertine zone and these zones above the travertine zone were formed during the second accumulation–laterization process, but the second laterization happened less intensively than the first. Of other major elements, FeO increases in content from the top to

Table 7
Chemical compositions (%) of the red clays in the Shangmanggang gold deposit, West Yunnan

Sample no.	SiO_2	FeO	Fe_2O_3	Al_2O_3	CaO	MgO	TiO_2	MnO	K_2O	Na_2O	H_2O	Total
S119	63.95	0.08	6.52	17.30	0.001	0.60	0.45	0.23	2.01	0.10	7.53	98.77
S118	70.23	0.07	5.73	15.10	0.20	0.70	0.33	0.05	2.19	0.09	4.46	99.16
S117	64.19	0.01	6.70	18.47	0.001	0.50	0.32	0.23	2.27	0.16	6.32	99.17
S116	65.47	0.60	7.55	15.37	0.38	0.60	0.75	0.20	2.64	0.14	5.42	99.12
S115	63.23	2.40	7.97	14.53	0.42	0.61	0.69	0.43	2.23	0.18	7.94	98.47
S114	59.95	0.98	6.77	15.93	0.41	0.69	0.74	0.17	2.23	0.20	9.90	97.97
S113	33.45	0.95	19.09	23.73	0.41	0.73	0.80	0.058	5.48	0.10	13.9	98.70
S112	63.69	0.71	8.38	16.08	0.41	0.59	0.69	0.17	2.41	0.13	5.79	99.05
S111	63.66	0.53	9.17	15.47	0.42	0.48	0.84	0.078	1.83	0.20	6.16	98.84
Altered rock[a]	68.35	0.29	7.33	11.20	1.11	1.31	0.70	0.01	2.25	0.06	5.17	98.45
Dolomite[b]	8.01	0.64	0.89	1.33	29.22	17.72	0.04	0.06	0.17	0.14	1.86	59.82
Detrital rock[c]	76.64	0.18	2.79	12.95	0.15	0.45	0.55	0.02	2.46	0.16	3.13	99.12

Analysis-testing Center of Institute of Geochemistry, Chinese Academy of Sciences.
[a] Mean value of altered rocks (7 samples).
[b] Mean value of Shazipo Formation dolomite (11 samples).
[c] Mean value of scraping rocks (8 samples).

Table 8
The selected parameters of chemical compositions

Sample no.	Coefficient of eluviation	Coefficient of laterization	SiO_2/Al_2O_3	Al_2O_3/Fe_2O_3	Fe^{2+}/Fe^{3+}
S119	28.039	5.067	6.284	4.162	0.014
S118	25.467	6.367	7.907	4.134	0.012
S117	27.258	5.769	5.908	4.324	0.007
S116	22.491	5.514	7.241	3.193	0.088
S115	21.343	5.553	7.398	2.859	0.338
S114	19.394	5.034	6.398	3.691	0.161
S113	6.522	1.584	2.396	1.950	0.055
S112	25.142	5.054	6.733	3.010	0.094
S111	21.319	5.077	6.996	2.646	0.064

Coefficient of eluviation, $SiO_2/(K_2O + Na_2O + CaO + MgO$; ratio of molecules); coefficient of laterization, $SiO_2/(Al_2O_3 + Fe_2O_3$; ratio of molecules).

bottom of the red clay profile, which shows that oxidation was weakened downward. FeO content reaches the maximum in the travertine zone, which implies that the travertine zone was ever under the reduced condition, was also under the paleowater table where oxidation, was weak during the second laterization process so that relatively high FeO content was induced in the upper eluvium zone. Much illite was accumulated in the top eluvium zone with an obvious increase of K_2O content by the effect of the travertine zone in the reduced environment. TiO_2 and MgO + CaO contents decrease upward from the bottom of the red clay profile. MnO arrives at the maximum in the bottom of the slope-wash zone.

7.1.2. Transport and enrichment of major elements in the red clays

Chemical compositions of the red clays were compared with sedimentary and altered rocks in the mining district in Table 7. Compared with clastic rocks of the middle Jurassic Mengga Formation, SiO_2 content is lower, whereas Al_2O_3, Fe_2O_3 and MnO contents are higher in the red clays. SiO_2 of clastic rocks of the middle Jurassic Mengga Formation was partly eluviated with slight enrichment of Fe and Al during laterization. SiO_2, Al_2O_3, and Fe_2O_3 of the red clays are higher in content than those of dolomite of the Low Permian Shazipo Formation. It was concluded that CaO and MgO of dolomite of Shazipo Formation were eluviated intensively with laterization, and then Al_2O_3 and Fe_2O_3 were enriched during the transformation from dolomite to the red clays, but enrichment of SiO_2 is resulted from relative increase of residuals after weathering. Compared with altered rocks, SiO_2, Na_2O, K_2O, CaO, and MgO are lower in content, whereas Al_2O_3, Fe_2O_3, and MnO are higher in the red clays owing to further weathering of altered rocks.

7.1.3. Laterization

Laterization parameters were calculated and shown in Table 8. The coefficient of laterization is 1.5 in the central part (eluvium zone) of the red clay profile, but is over 5 in the other zones. Therefore, the degree of laterization is low in the whole red clay profile, and

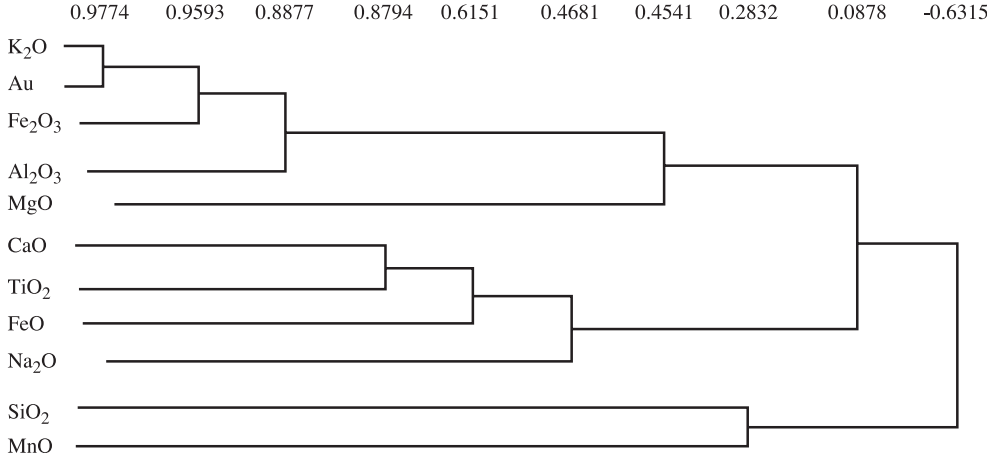

Fig. 5. R-type clustering analysis of gold and major elements in the red clays.

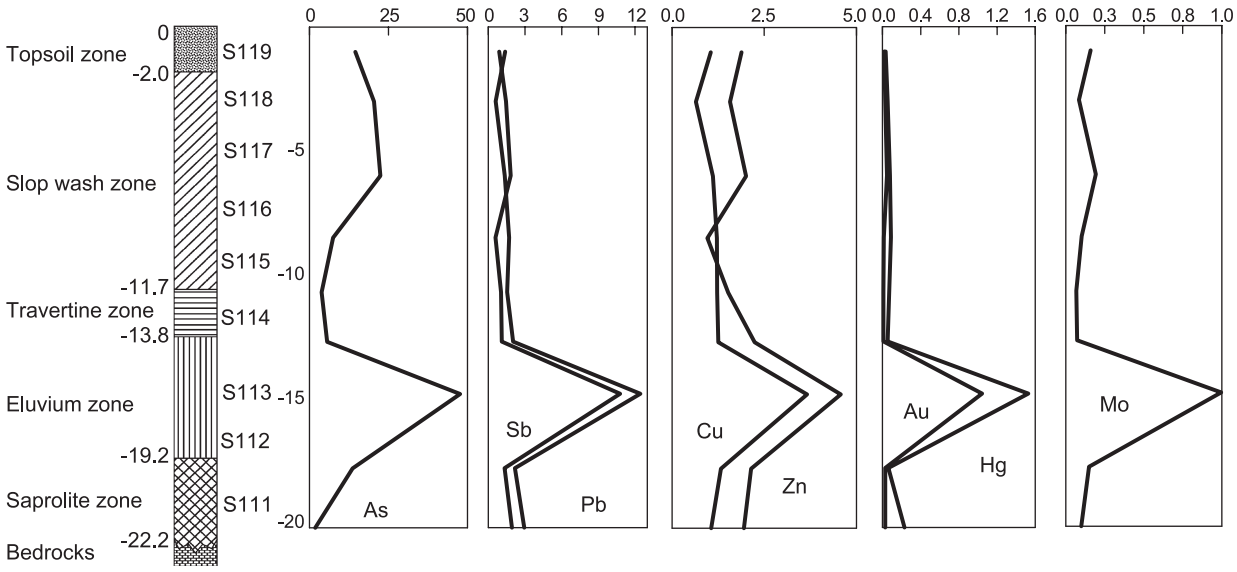

Fig. 6. Variations of (100 × trace elements)/Ti in the red clay profile.

desilification is strong only in the eluvium zone. The coefficient of eluviation varies from high to low then to high with increasing depth, which likely reflects that laterization happened twice in the red clay profile. The ratio of SiO_2 to Al_2O_3 is over 5 in the other zones except in the eluvium zone, which indicates that the degree of desilification and Al accumulation is low, but the ability of desilification and Al accumulation is strong only in the eluvium zone. The ratio of Al_2O_3 to Fe_2O_3 is slightly variable from 1.9 to 4.4 in the red clay profile, showing no obvious separation of Fe from Al. The ratio of Fe^{2+} to Fe^{3+} is high in the travertine zone and the contact between the travertine zone and the slope-wash zone, 0.161 and 0.338, respectively. The ratio is low in the central slope-wash zone (S117) and central eluvium zone (S113), 0.007 and 0.055, respectively. Fe^{2+}/Fe^{3+} ratio in the red clay profile indicates that the eluvium and slope-wash zones were

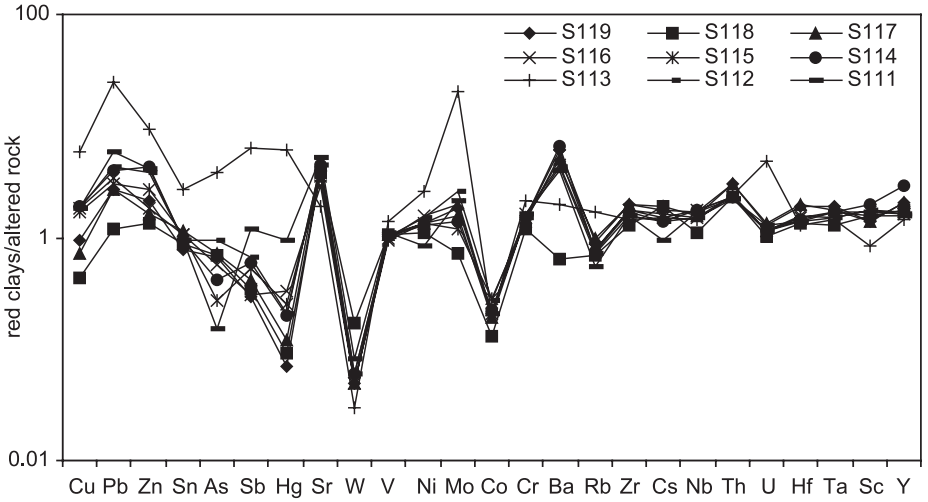

Fig. 7. Diagram of trace elements of the red clays in the Shangmanggang gold deposit, normalized with altered rocks.

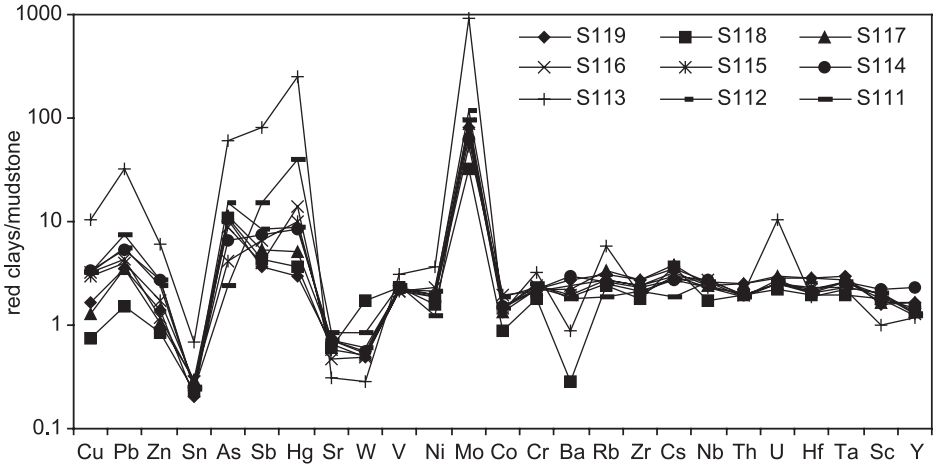

Fig. 8. Diagram of trace elements of the red clays in the Shangmanggang gold deposit, normalized with mudstone of Middle Jurassic Mengga Formation.

in the aerobic environments in contrast with the other zones. Consequently, laterization occurred twice in the red clay profile, and the degree of laterization was more intense than in the other zones.

On the whole, SiO_2 content is high, and desilification is not strong in the red clay profile. Fe and Al are accumulated unobviously, and the degree of laterization is low, except in the eluvium zone.

7.1.4. Correlation between gold and major elements

Gold content varies from low to high and then to low with increasing depth, and is the highest in the eluvium zone. Al_2O_3, Fe_2O_3, and K_2O contents vary in accordance with gold (Fig. 3). As Fig. 5 shows, correlative coefficient of gold with K_2O is 0.9774, which suggested that illite is a main mineral containing gold. In addition, gold is well correlated with

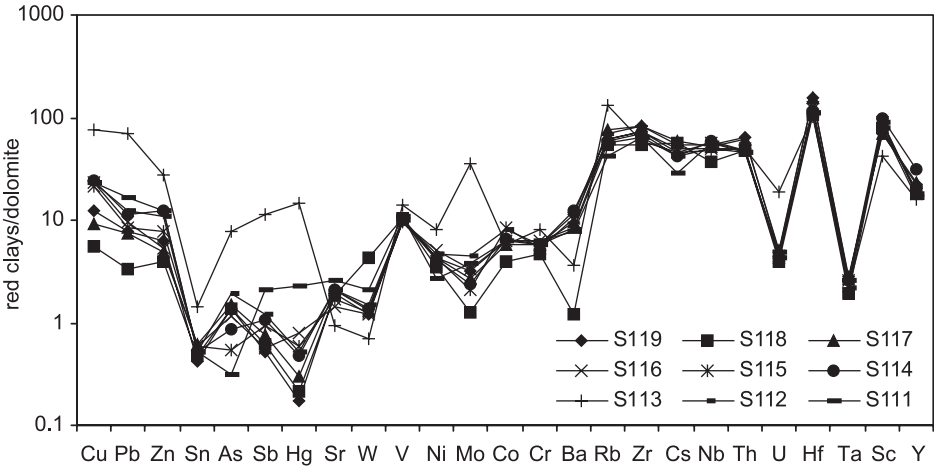

Fig. 9. Diagram of trace elements of the red clays in the Shangmanggang gold deposit, normalized with dolomite of the Lower Permain Shazipo Formation.

Fe_2O_3 and Al_2O_3 with correlative coefficients of 0.9593 and 0.8877, respectively, implying close relations of gold with goethite and clay minerals. More importantly, the above results indicate that Au, K, Fe, and Al are a group of coexisting elements in the red clays. Gold has not a close correlation with other major elements with the exception of Fe, K, and Al.

7.2. Trace element geochemistry

7.2.1. Vertical distribution of trace elements in the red clay profile

The absolute contents of trace elements in the red clays cannot exactly reflect the rules of their mobility because of mass depletion or volume decrease of the weathering crust in the process of laterization. Ti, Zr, Th, and Al were used to correct the contents of other elements (Braun et al., 1993; Braun et al., 1998). Titanium belongs to immobile elements during weathering and can effectively exist in secondary oxides after weathering (Braun et al., 1993; Nesbitt, 1979; Nesbitt and Markovics, 1997). Titanium content is usually high in the weathering profile and less different among samples as compared with Zr and Th. So Ti is used to evaluate the mobility of other elements.

Au, Hg, Sb, Mo, Pb, Cu, Zn and As have similar characteristics in the red clay profile (Fig. 6). Their contents are very high in the eluvium zone, but low in the other zones. These results above indicate that gold was mobilized, transported, and enriched near the eluvium zone during the formation of the SMG red clay-type gold deposit. Au, Hg, Sb, As, and Mo are a group of coexisting elements, an indicator of mineralization at low temperature under hypergenic conditions.

7.2.2. Normalization characteristics of trace elements in the red clays

Compared with sedimentary and altered rocks, trace elements of the red clays in the SMG red clay-type gold deposit have the following characteristics as Figs. 7, 8 and 9 show.

As, Sb, and Hg in the red clays are lower in content than those in the altered rocks and slightly lower than in the dolomite but higher than in clastic rocks, probably provided by the altered rocks. Nb, Ta, Zr, Hf, U, and Th in the red clays do not have an obvious change as compared with those in altered rocks and clastic rocks, whereas they are intensively enriched as compared with dolomite, which reflects that the red clays were formed from the weathering of many altered rocks and clastic rocks with little dolomite. Sr and Ba contents in the red clays are higher than in the altered rocks but lower than in the clastic rocks, indicating that Sr and Ba in the red clays were provided by clastic rocks and dolomite.

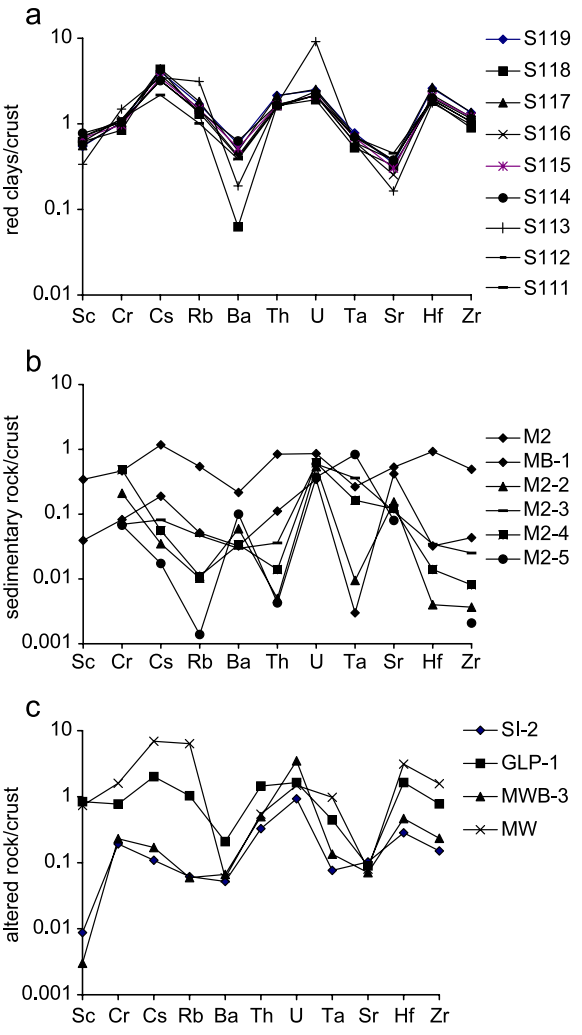

Fig. 10. Diagrams of crust abundance-normalized large-ion lithophile elements from the red clays (a), sedimentary rocks (b), altered rocks (c) in the SMG red clay-type gold deposit (Liu, 1999).

Rb and Cs in the red clays could be provided by the altered rocks, because Rb and Cs in the red clays are slightly higher than those in the altered rocks but obviously higher than in the dolomite. Pb and Zn contents in the red clays are slightly higher with lower Cu content as compared with in the altered rocks and apparently higher with higher Cu content than in the dolomite, implying that Pb, Zn, and Cu in the red clays came from the altered rocks. Ni, Cr, V, and Sc in the red clays are slightly higher than those in the altered rocks and clastic rocks but obviously higher than in the dolomite. These elements in the red clays could come from the altered rocks and clastic rocks. W content in the red clays is lower than in the altered rocks and clastic rocks. Sn in the red clays is lower than in the clastic rocks. Mo in the

Table 9
REE contents (ppm) and selected parameters in the red clays, altered rocks, sedimentary rocks, and magmatic rocks in the Shangmanggang gold deposit

Sample no.	Lithology	La	Ce	Pr	Nd	Sm	Eu	Gd	Tb	Dy	Ho	Er	Tm	Yb	Lu	ΣREE
S119	Red clay	49.6	102	11.3	41.2	7.62	1.57	6.94	1.09	6.46	1.28	3.87	0.562	3.81	0.582	239
S118	Red clay	39.6	76.7	9.17	34.1	6.59	1.44	6.13	0.970	5.77	1.18	3.44	0.508	3.49	0.513	190
S117	Red clay	47.8	98.5	10.9	39.6	7.70	1.62	7.31	1.09	6.69	1.37	3.98	0.608	4.06	0.583	232
S116	Red clay	42.3	90.6	9.71	35.2	7.13	1.42	6.14	0.950	5.62	1.13	3.32	0.510	3.39	0.520	208
S115	Red clay	44.2	94.3	9.88	36.1	6.89	1.19	5.56	0.850	5.42	1.00	3.06	0.470	3.09	0.490	212
S114	Red clay	58.0	100.	14.0	52.2	11.2	2.49	11.0	1.66	9.52	1.77	5.01	0.740	4.44	0.650	273
S113	Red clay	46.3	83.8	9.46	32.6	4.69	0.880	3.96	0.620	4.02	0.780	2.79	0.420	2.92	0.450	194
S112	Red clay	42.2	88.9	9.49	34.4	6.55	1.30	5.91	0.890	5.38	1.06	3.42	0.530	3.12	0.460	204
S111	Red clay	42.9	88.6	9.55	35.0	6.78	1.28	5.26	0.880	5.11	0.980	3.14	0.440	3.10	0.470	203
SI-2	Silicification-altered rock	8.51	19.0	2.28	8.61	1.36	0.284	1.81	0.369	2.53	0.525	1.54	0.220	1.15	0.166	48.3
GLP-1	Silicifiation–pyritization mudstone	31.2	69.6	7.99	33.6	6.72	0.993	5.92	0.883	5.33	1.11	3.25	0.447	3.00	0.414	170
MWB-3	Silicification-altered rock	9.36	19.0	2.07	7.23	0.976	0.168	0.679	0.141	1.05	0.247	0.713	0.123	0.833	0.110	42.7
MWB	Kaolinitization–pyritization-altered rock	3.45	8.49	1.18	5.07	0.964	0.232	1.38	0.430	3.41	0.887	2.67	0.467	3.42	0.452	32.5
M2	Mengga Formation mudstone	18.8	40.0	4.79	19.5	4.47	0.958	4.68	0.686	4.07	0.800	2.29	0.332	2.21	0.303	104
MB-1	Shazipo Formation dolomite	4.01	8.31	0.985	3.91	0.573	0.116	0.755	0.106	0.697	0.142	0.389	0.051	0.312	0.023	20.4
M2-2	Brecciated dolomite	0.15	0.446	0.058	0.489	0.323	0.090	0.325	0.046	0.272	0.045	0.108	0.019	0.098	0.012	2.48
M2-3	Gray dolomite	1.01	2.21	0.264	0.977	0.190	0.049	0.232	0.033	0.175	0.044	0.104	0.016	0.074	0.014	5.40
M2-4	Muddy dolomite	0.529	1.09	0.125	0.528	0.162	0.037	0.147	0.018	0.120	0.021	0.054	0.010	0.049	0.006	2.89
M2-5	Coarse crystal dolomite	0.184	0.322	0.042	0.199	0.044	0.020	0.049	0.010	0.067	0.012	0.028	0.004	0.022	0.004	1.01
FH-1	Peridotite	0.507	0.183	0.053	0.167	0.013	0.005	0.015	0.002	0.007	0.0001	0.005	0.001	0.009	0.002	0.972
XS-7	Basic rock vein	0.143	0.244	0.029	0.107	0.013	0.005	0.019	0.003	0.014	0.003	0.009	0.002	0.008	0.002	0.600
YSS-2	Lamprophyre dyke	60.8	121	12.9	49.0	8.36	2.52	6.76	0.940	5.18	0.884	2.50	0.322	2.43	0.289	273

Institute of Geochemistry, Chinese Academy of Sciences (ICP-MS).

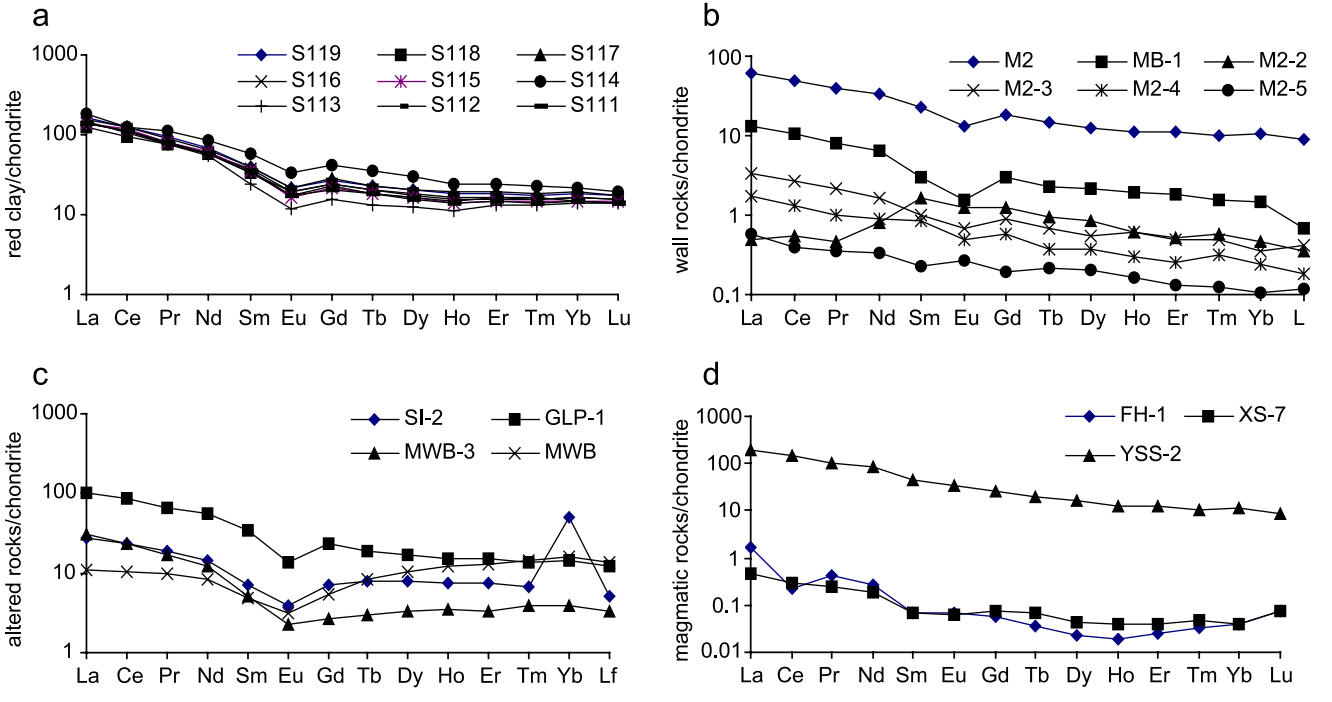

Fig. 11. Chondrite-normalized REE patterns of the red clays (a), sedimentary rocks (b), altered rocks (c), and magmatic rocks (d) in the SMG red clay-type gold deposit.

red clays is slightly higher in content than that in the altered rocks and dolomite, obviously higher than in the clastic rocks. W and Sn could come from the altered rocks and clastic rocks, but Mo could be provided by other type of rocks.

Moreover, crust-normalized patterns of the red clays are similar to those of the altered rocks and the Mengga Formation mudstones. They are rich in Cs and U, poor in Ba and Sr, showing obvious differences from the Shazipo Formation dolomite (Fig. 10).

These characteristics of trace elements show that the red clays are mainly the weathering products of the altered rocks and clastic rocks with entry of little dolomite.

7.3. REE geochemistry

7.3.1. REE contents and chondrite-normalized REE patterns

Chondrite-normalized patterns of red clay samples (Wang et al., 1989) are similar (Table 9; Fig. 11). The total contents of the red clays vary from 189.6 to 272.9 ppm. LREE/HREE is from 6.9 to 11.1; CeN/YbN, from 5.7 to 7.9. The LREE pattern curve is much steep, whereas HREE pattern curve is relatively smooth. δEu ranges from 0.55 to 0.68, with negative Eu anomaly. δCe ranges from 0.82 to 1.04, with less remarkable negative Ce anomaly. These results indicate that REE fractionation took place during laterization and resulted in relatively high LREEs and low HREEs in content in the weathered residues (Braun et al., 1990). LREE fractionation is obvious but HREE fractionation is unobvious. Eu is lost and Ce is relatively stable.

The REE patterns of the red clays are similar to those of altered rocks and Mid-Jurassic Mengga Formation rocks, and partly similar to those of the Shazipo Formation dolomite, different from those of magmatic rocks in both mining district and its surroundings. In addition, the characteristic parameters for the red clays are similar to those of both sedimentary rocks and altered rocks: LREE/HREE>1, $Ce/Yb_N>1$, δEu < 1, δCe = 1 ± . But there exist certain differences too. For example, ΣREE is obviously higher than that of sedimentary and altered rocks probably as a result of weathering and leaching (Li, 1986; Figs. 11 and 12).

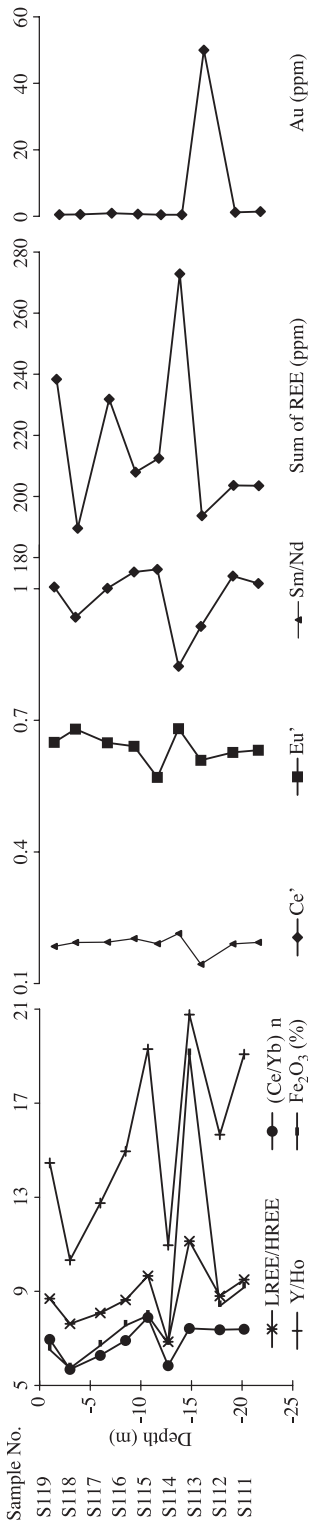

Fig. 12. Variation of the selected parameters in the red clay profile of the SMG red clay-type gold deposit.

7.3.2. Discussion of parameters

There is no correlation of Au with REE in the red clay profile. Intense REEs fractionation occurs where gold content is relatively high because of the effect of laterization under the relatively aerobic conditions. Additionally, the variation of Fe_2O_3 is generally consistent with those of LREE/HREE, (Ce/Nb)*n* and Y/Ho. Consequently, Fe_2O_3 has a close relationship with REE. Sm/Nd does not fluctuate obviously in the other zones except in the eluvium zone. Sm and Nd are slightly mobile only in the eluvium zone; the mobility of Sm is lower than that of Nd. Y and Ho are of certain mobility in the red clay profile, reflecting that there are differences among HREEs (Fig. 12).

Ce anomaly reflects the redox environment of rock formation. Ce has two valence states: Ce^{2+} and Ce^{4+}. Ce^{3+} is easily converted to $Ce^{4+}(CeO_2)$ in the upper parts of the red clay profile and is preserved in both eluvium and slope-wash zones. As a result, Ce is lower in the lower parts of the profile. In fact, δCe is about 1 in all red clay samples, only in sample S114 is δCe equal to 0.82. It is concluded the sample S114 was possibly deposited in a reductive and humid environment. δEu is below 0.7 in the red clay profile with obvious negative Eu anomaly because of transport and accumulation of Ca-bearing minerals (Fig. 12).

8. Discussion of source materials

8.1. Source of the red clays

Characteristics of both macroscopical geology and elemental geochemistry show the following:

(1) There are only a few lamprophyre dykes in the Yangshishan ore run of the SMG mining zone. Mid-Jurassic Mengga Formation and Lower Permian Shazipo Formation are exposed in this mining district. The red clays exist on the karst surface of the Shazipo Formation, where the Carlin-type gold deposits and altered rocks containing gold have been discovered. The red clay-type and Carlin type gold deposits are controlled by the SMG fault.
(2) Migration and accumulation of the major elements indicate that the red clays are mainly formed on the basis of the Mid-Jurassic Mengga Formation through laterization. Secondly, altered rocks, as well as Carlin type gold deposits and Shazipo Formation dolomite, provides a small quantity of materials for the formation of the red clays.
(3) Like large-ion lithophile-ion elements, REE patterns can be usually used to explore the ore-forming sources (Pan, 1999). Large-ion lithophile element patterns of the red clays are similar to those of the Mid-Jurassic Mengga Formation and altered rocks, but different from those of the Lower Permian Shazipo Formation. These characteristics indicate that the red clays have inherited the element compositions of altered rocks and the Mengga Formation. Few fractions from the Shazipo Formation are probably involved in mineralization. Normalization characteristics of trace elements in the red clays also demonstrate the above results.
(4) REE patterns of the red clays are consistent with those of altered rocks and sedimentary rocks, and their parameters are very similar. It is concluded that the REE in the red clays were derived from altered rocks and sedimentary rocks, independent of magmatic rocks.

8.2. Source of gold

As compared with the mean value of the crust (Liu et al., 1999), gold is more or less enriched in sedimentary rocks and magmatic rocks. But it is impossible for both of them to be the main source of ore-forming materials of the SMG red clay-type gold deposit (Table 3). First, as compared to the abundance of the crust, they have high contents of gold, but as compared to altered rocks and the red clays, their gold contents are very low. Secondly, the formation of the SMG red clay-type gold deposit requires a large amount of sedimentary and magmatic rocks. In fact, the SMG red clay-type gold deposit is obviously controlled by the SMG fault, and there are minor sedimentary rocks and magmatic rocks in the district. Consequently, the altered rocks containing high contents of gold are the main source materials of the SMG red clay-type gold deposit.

In addition, trace element characteristics of the red clay profile indicate that Au, Hg, Sb, Mo, Pb, Cu, Zn, and As are closely associated with one another, and

the red clays inherit the composition of trace element in the altered rocks, further demonstrating that the altered rocks containing high contents of gold are the main source material of the SMG red clay-type gold deposit.

Acknowledgements

This study is financially supported by the National Natural Science Foundation of China (49873021). We thank Prof. Rudy Swennen, Dr. Alan W. Mann, and Dr. M.L. Costa for many helpful comments and language improvements.

References

Braun, J.J., Pagel, M., Muller, J.P., Bilong, P., Michard, A., Guillet, B., 1990. Cerium anomalies in lateritic profiles. Geochimica et Cosmochimica Acta 54, 781–795.

Braun, J.J., Pagel, M., Herbillon, A., Rosin, C., 1993. Mobilization and redistribution of REEs and thorium in a syenitic lateritic profile: a mass balance study. Geochimica et Cosmochimica Acta 57, 4419–4434.

Braun, J.J., Viers, J., Dupké, B., Polve, M., Ndam, J., Muller, J.P., 1998. Solid/liquid REE fractionation in the lateritic system of Goyoum, East Cameroon: the implication for the present dynamics of the soil covers of the humid tropical regions. Geochimica et Cosmochimica Acta 62 (2), 273–299.

Carvalho, I.G., Mestrinho, S.S.P., Fontes, V.M.S., Goel, O.P., Souza, F.A., 1991. Geochemical evolution of laterites from two areas of the semiarid region in Bahia State, Brazil. Journal of Geochemical Exploration 40, 385–411.

Chen, L.A., 1999. Major element geochemistry and laterization of Laowanchang lateritic gold deposit in Qinglong, Guizhou province. Guizhou Geology 16 (4), 307–314 (in Chinese with English abstract).

Chen, D.J., Yang, M.S., 1998. Geological characteristics of lateritic gold deposits in South China. Mineral Resources and Geology (2), 5–6 (in Chinese with English abstract).

Colin, F., Vieillard, P., 1991. Behavior of gold in the lateritic equatorial environment: weathering and surface dispersion of residual gold particles, at Dondo Mobi, Gabon. Applied Geochemistry 6, 279–290.

Costa, M.L., 1993. Gold distribution in lateritic profiles in South American, Africa and Australia: application to geochemical exploration in tropical regions. Journal of Geochemical Exploration 37 (1–3), 143–163.

Costa, M.L., Araújo, E.S., 1996. Application of multi-element geochemistry in the Au–phosphate-bearing lateritic crusts for identification of their parent rocks. Journal of Geochemical Exploration 57, 257–272.

Davies, T.C., Friedrich, G., Wiechowski, A., 1989. Geochemistry and mineralogy of laterites in the Sula Mountains greenstone belt, Lake Sonfon gold district, Sierra Leone. Journal of Geochemical Exploration 32, 75–98.

Davy, R., El-ansary, M., 1986. Geochemical patterns in the laterite profile at the Boddington gold deposit, Western Australia. Journal of Geochemical Exploration 26, 119–144.

Freyssinet, Ph., Zeegers, H., Tardy, Y., 1989a. Morphology and geochemistry of gold grains in lateritic profiles of southern Mali. Journal of Geochemical Exploration 32 (1), 17–32.

Freyssinet, Ph., Lecomte, P., Edimo, A., 1989b. Dispersion of gold and base metals in the Mborguene lateritic profile, east Cameroon. Journal of Geochemical Exploration 32, 99–116.

Freyssinet, Ph., Lawrance, L.M., Butt, C.R.M., 1990. Geochemistry and morphology of gold in lateritic profiles in savanna and semi-arid climates. Chemical Geology 84 (1–4), 61–63.

Glasson, M.J., Lehne, R.W., Wellmer, F.W., 1988. Gold exploration in the Callion area, eastern Goldfields, Western Australia. Journal of Geochemical Exploration 31, 1–19.

Gleeson, C.F., Poulin, R., 1989. Gold exploration in Niger using soils and termitaria. Journal of Geochemical Exploration 31, 253–283.

He, W.J., 1998. Geological features, metallogenic conditions and exploration perspective of laterite gold deposits in western Jiangxi. Mineral Resources Geological 12 (5), 329–334 (in Chinese with English abstract).

Heylmun, E.B., 1986. Nickel–iron–gold laterites in Washington State. California Mining Journal 56 (2), 55–57.

Hong, J.Y., Du, Z.M., Lu, S.H., Xie, G.Z., 1996. Geological condition of metallozation of southern Hunnan. Journal of Central South University of Technology 27 (5), 511–515 (in Chinese with English abstract).

Jiang, N.S., 1999. Geological characteristics and factors controlled of laterite gold deposits in southern Hunan. Hunan Geology 18 (2,3), 79–83 (in Chinese with English abstract).

Jin, J.F., Ni, S.J., Liu, X.F., 1995. Low temperature geochemistry behaviors of thermal liquids after mineralization and hypergenic solution of micro-fine and dip-dye type gold deposit among Yunnan, Guizhou and Guangxi–Research of transformation mechanism of original ore minerals to oxidated ore minerals. Report of imbursing Item of State Key Laborary of Ore Deposit Geochemistry, Institute of Geochemistry, Chinese Academy of Sciences, Guiyang (series number, 9308).

Lecomte, P., Colin, F., 1989. Gold dispersion in a tropical rainforest weathering profile at Dondo Mobi, Gabon. Journal of Geochemical Exploration 32, 285–301.

Li, C.N., 1986. Trace Element and its Application to Petrology. Teaching and Research Section of Petrology, Wuhan College of Geology, Wuhan, pp. 36–40. In Chinese.

Li, S.S., 1993. Geological feature and genesis of lateritic gold deposit in Shewushan, Hubei. Geological Prospectives 1, 12–15 (in Chinese with English abstract).

Li, Z.Q., 1998. Geological Features and metallogenic conditions of laterite gold deposits in Yunnan. Mineral Resources and Geology 12 (3), 160–166 (in Chinese with English abstract).

Liu, T.F., 1996. Geological feature and exploration of lateritic gold

deposit in Shewushan, Hubei. Gold Geology 2 (3), 25–30 (in Chinese with English abstract).

Liu, Y.P., 1999. Mettalogenic theories and prospecting of lateritical gold deposits in Guizhou. Geological Exploration for Non-Ferrous Metals 8 (6), 353–358 (in Chinese with English abstract).

Liu, B.G., Lu, D.F., Cai, X.P., 1999. Research of Gold Deposits in Western Yunnan and Sichuan. China Ocean Press, Beijing, pp. 119–128. In Chinese.

Lu, B.X., 1994. Future of prospecting of lateritical gold deposits in Yunnan. Geological Science and Technology Information Yunnan (2), 1–3 (in Chinese with English abstract).

Mann, A.W., 1984. Mobility of gold and silver in lateritic weathering profiles: some observations from Western Australia. Economic Geology 79, 38–49.

Narayanaswamy, Krishnakumar, N., 1996. Geology and geochemistry of lateritic gold occurrences in Nilambur Valley, Kerala and their economic potential. Indian Mineralogist 30, 31–47.

Nesbitt, H.W., 1979. Mobility and fractionation of rare earth elements during weathering of a granodiorite. Nature, 206–210.

Nesbitt, H.W., Markovics, G., 1997. Weathering of granodioritic crust, long-term storage of elements in the weathering profiles, and petrogenesis of siliciclastic sediments. Geochimica et Cosmochimica Acta 61 (8), 1653–1670.

No.4 Geological Party of HBGMR, 1994. The geological characteristics of laterite gold ore of Shewushan type in Hubei. Hubei Geology 2 (8), 25–33 (in Chinese with English abstract).

Pan, J.Y., 1999. Geochemistry and Mechanism of Metallization of Copper and Multi-Metal Deposit Zones. Institute of Geochemistry, Chinese Academy of Sciences, Guiyang. (In Chinese with English abstract).

Porto, C.G., Hale, M., 1995. Gold redistribution in the stone line lateritic profile of the Pose Deposit, central Brazil. Economic Geology 90 (2), 308–321.

Porto, C.G., Hale, M., 1996. Mineralogy, morphology and chemistry of gold in the stone line lateritic profile of the Posse Deposit, central Brazil. Journal of Geochemical Exploration 57 (1–3), 115–125.

Qiu, Z.L., Chen, F.X., 1998. Geological features and analysis of ore-forming mechanism for lateritic gold deposit in somewhere in Jiangsu province. Jiangsu Geology 22 (1), 27–30 (in Chinese with English abstract).

Santosh, M., Omana, P.K., 1991. Very high purity gold from lateritic weathering profiles of Nilambur, southern India. Geology 19, 746–749.

Shcherbakov, Y.G., Nguyen, C.J., Nguen, V.F., 1992. Gold in laterites of Vietnam. Russian Geology and Geophysics 33 (5), 75–81.

Taylor, G.H., Coste, B., Lambert, A., Zeegers, H., 1989. Geochemical signature (bedrock and saprolite) of gold mineralization and associated hydrothermal lateration at Dorlin, French Guyana. Journal of Geochemical Exploration 32, 59–60.

Wang, R.H., 1999. Basic types and prospecting of lateritical gold deposits in Guangxi. Geological Exploration for Non-Ferrous Metals 8 (6), 687–689 (in Chinese with English abstract).

Wang, Z.G., Yu, X.Y., Zhao, Z.H., 1989. Geochemistry of Rare Earth Elements. Science Press, Beijing, p. 93. In Chinese.

Webster, J.G., Mann, A.W., 1984. The influence of climate, geomorphology and primary geology on the supergene migration of gold and silver. Journal of Geochemical Exploration 22, 21–42.

Zang, W.S., Fyfe, W.S., 1993. A three-stage genetic model for the Igarape Bahia lateritic gold deposit, Carajas, Brazil. Economic Geology 88 (7), 1768–1779.

Zhang, X.S., 1998. Mettalogenisis of the Beiya Lateritic gold deposit and its prospecting, West Yunnan. Geological Exploration for Non-Ferrous Metals 7 (3), 156–159 (in Chinese with English abstract).

Zhao, X.Y., Zhang, Y.Y., 1990. Clay Minerals and its Analysis. China Ocean Press, Beijing, pp. 71–83. In Chinese.